Drug Deliv. and Transl. Res. (2017) 7:16–26
DOI 10.1007/s13346-016-0328-5

ORIGINAL ARTICLE

Novel in situ forming hydrogel microneedles for transdermal drug delivery

Arunprasad Sivaraman[1] · **Ajay K. Banga**[1]

Published online: 25 August 2016

Abstract Novel in situ forming hydrogel microneedles were evaluated for transdermal drug delivery using a biocompatible non-ionic triblock amphiphilic thermosensitive copolymer. The transition property of poloxamer from solution at room temperature to gel at skin temperature (32 °C) was utilized in preparation of in situ forming hydrogel microneedles. Methotrexate has been used to treat solid tumors, but because of its narrow safety margin, it requires sustained delivery within the therapeutic window. Formulations with and without poloxamer at different methotrexate concentrations were prepared and evaluated for drug permeation across skin using vertical Franz diffusion cell for 72 h. Sol-gel transition, skin resistance and thickness, microneedles geometry, microchannel depth, shape, formation and uniformity, viscoelasticity of skin, and in vitro drug permeation were characterized and tested. An average cumulative drug amount of 32.2 ± 15.76 and 114.54 ± 40.89 μg/cm^2 for porcine ear skin and 3.89 ± 0.60 and 10.27 ± 6.98 μg/cm^2 for dermatomed human skin from 0.2 % *w/w* and 0.4 % *w/w* methotrexate formulations was delivered by the in situ forming hydrogel microneedles. These in situ hydrogel microneedles embedded within the porated site of the skin provided a steady and sustained drug delivery.

Keywords Microneedle · biocompatible · poloxamer · In situ hydrogel · transdermal drug delivery · methotrexate

✉ Ajay K. Banga
banga_ak@mercer.edu

[1] College of Pharmacy, Department of Pharmaceutical Sciences, Mercer University, Atlanta, GA, USA

Introduction

Transdermal drug delivery provides a promising alternative to oral and parenteral delivery because of the advantages such as avoidance of first pass effect, patient acceptability, painless delivery, and easy discontinuation [1]. Generally, transdermal patches and gels are considered as passive delivery techniques while microneedles, iontophoresis, sonophoresis, and ultrasound are considered as enhanced delivery techniques. The passive transdermal systems are confined only to drugs with low molecular weight, moderate lipophilicity, and low melting point and are not suitable for macromolecules [2]. Transdermal delivery of macromolecules requires enhanced techniques, and for the past few years, significant research efforts have been focused on microneedle-based transdermal delivery systems.

The stratum corneum with an approximate thickness of 10 to 15 μm is the main barrier for drug flux through the skin. The insertion of microneedles causes reversible disruption to the stratum corneum and creates microchannels in the skin [1–3]. The microneedles are minimally invasive and tiny needle-like structures with a length ranging from 250 μm typically up to 1500 μm [2, 4]. Solid, coated, dissolving, hollow, and hydrogel-forming are the five different types of microneedles that have been investigated [4].

"Poke with patch" was the first strategy used for solid microneedle-mediated transdermal drug delivery [5]. In this technique, the drug formulation was applied after removal of microneedle from the skin and the drug delivery occurred by passive diffusion [2]. Materials such as silicon, maltose, metals, and polymers are generally used to prepare solid microneedles [6–8]. Coated microneedles that are typically made of silicon, metal, or polymers provide rapid onset of drug delivery by allowing the drug to dissolve from the coated surface of microneedles after insertion into the skin [5, 9].

However, this technique is feasible only for potent drug molecules as it allows only tiny surface area for drug coating. Transcutaneous vaccination using these coated microneedles has been extensively researched [10].

The dissolving microneedles form aqueous microchannel after insertion into the skin due to influx of skin interstitial fluid [1, 2]. Polymers and biopolymers such as polylactic acid (PLA), polyglycolic acid (PGA), polylactic-*co*-glycolic acid (PLGA), polyvinylpyrrolidone (PVP), poly(vinylpyrrolidone-*co*-methacrylic acid) (PVP-MAA), poly(methyl vinyl ether-maleic anhydride), sodium hyaluronate, chondroitin sulphate, and carbohydrates are generally used in preparation of dissolving microneedles [11, 12]. Balance between drug loading and mechanical strength of the microneedle, drug stability during fabrication, and residual polymer within the skin are few of the limitations with dissolving microneedles. Use of biodegradable and water soluble polymers can eliminate the concern of residual biohazardous waste within the skin [12, 13]. Significant attention has been focused towards investigation of dissolving microneedles [14].

Hollow microneedles typically made of silicon, metal, glass, or ceramic deliver drug by the process of diffusion as well as pressure through the bore opening [15–17]. The length and inner diameter can influence the rate of drug delivery [18]. Clogging of bore opening due to skin deformation and volume loss can happen during application of hollow microneedles [19–21]. However, these limitations can be overcome by using applicator made of non-flexible materials with an improved accuracy, precision, and reproducibility [22]. Hydrogel-forming microneedles, an aqueous blend of polymeric material, forms by imbibition of interstitial fluid from the skin. Poly (methylvinylether/maleic acid) and poly (ethyleneglycol) are used in preparation of hydrogel-forming microneedles. Drug delivery from these microneedles can be controlled by altering the crosslink density of the polymer [23].

For the first time, "in situ forming hydrogel microneedles" were investigated in our study using a non-ionic triblock amphiphilic thermosensitive copolymer, poloxamer. This copolymer is available as Pluronic® F127 or Kolliphor® P 407 and consists of ethylene oxide (EO) and propylene oxide (PO) blocks in the arrangement of EO-PO-EO with a molecular weight of around 12,600 daltons and is characterized by its non-ionic and amphiphilic properties [24–26]. One of the significant properties is the sol-gel transition of this polymer at skin (32 °C) or human body (37 °C) temperature. The aqueous solution of this polymer remains fluid at room temperature and transitions to gel above room temperature [27]. The dehydration of PO units causes the polymer to aggregate and results in formation of micelles eventually causing gelation [28]. Increase in temperature of the polymer solution causes the PO units to form a core where the water-insoluble molecules can be encapsulated within this hydrophobic core and leaving the hydrophilic tails of EO units around the hydrophobic core [29–32]. This copolymer has been approved as an inactive ingredient by the FDA for topical, intravenous, oral solution, inhalation, and ophthalmic preparations [24].

In our study, the sol-gel transition property of this polymer has been utilized in creating in situ forming hydrogel microneedles. The skin was microporated using 500-μm-length maltose microneedles stacked in three rows, as shown in Fig. 1, followed by application of poloxamer-based drug formulation where the solution flowed inside the created microchannels, transitioned into gel at skin temperature, and attained the shape of microneedle. These in situ formed hydrogel microneedles embedded within the skin delivered the encapsulated drug in a sustained fashion. Figure 2 provides a schematic representation about formation and delivery of drug from the in situ formed hydrogel microneedles. Hydrophilic drug molecules and macromolecules can be incorporated in these type of in situ formed hydrogel microneedles. Methotrexate (2, 4-diamino-*N* 10- methyl propylglutamic acid) with a molecular weight of 454.5 g/mol, pKa values of 3.8, 4.8 and 5.6, log P of −1.85 (hydrophilic) has been used in treatment of cancer, rheumatoid arthritis, and psoriasis; however, it is associated with limitations such as poor pharmacokinetic profile, narrow safety margin, and toxicity with increased dosing [3, 33]. The relatively high molecular weight and hydrophilicity limit the use of this drug in transdermal delivery. In our study, we incorporated methotrexate as a model drug in the in situ formed hydrogel microneedles, characterized, and evaluated for transdermal delivery.

Materials and methods

Formulation

Methotrexate (Sigma-Aldrich, St. Louis, MO) was dissolved in pH 7.4 phosphate buffer solution (1:3) (Phosphate buffer saline, Fisher Scientific, Fairlawn NJ) with 20 % *w*/*v*

Fig. 1 Proscope image of maltose microneedles

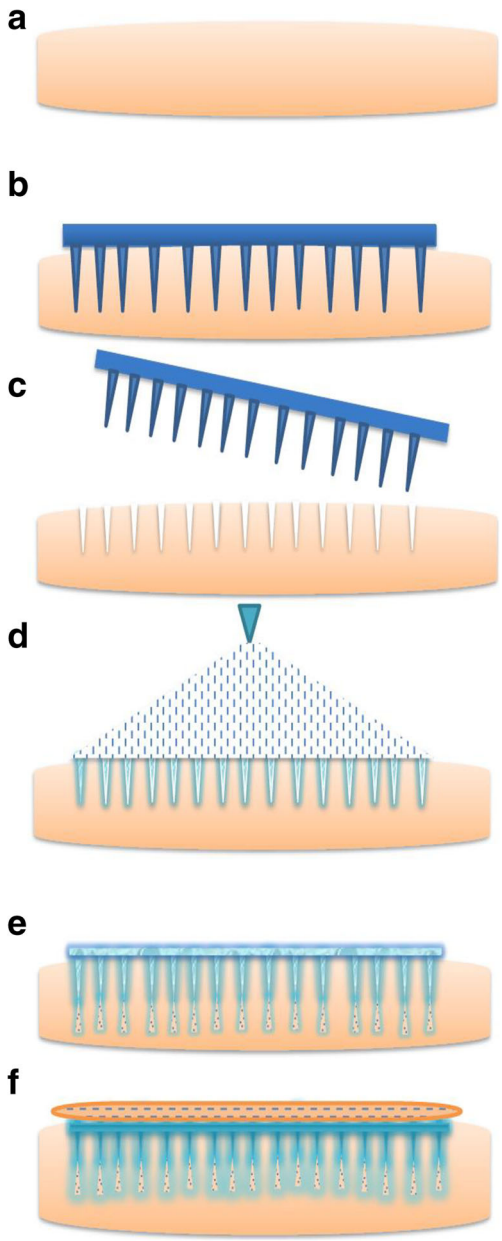

Fig. 2 Schematic representation of formation and delivery of drug from in situ forming hydrogel microneedles (**a**). Non-porated skin (**b**), skin porated with maltose microneedles (**c**), pore formation after removal of maltose microneedles (**d**), application of drug-poloxamer solution (**e**). Flow of drug-poloxamer solution into the porated site of skin (**f**) transition of drug-poloxamer solution to gel state at skin temperature (32 °C) to form in situ hydrogel microneedles

poloxamer (Pluronic® F127, BASF – The Chemical Company, Tarrytown, NY) solution. Four formulations with two methotrexate (0.2 % *w*/*w* and 0.4 % *w*/*w*) concentrations with poloxamer and without poloxamer (non-poloxamer) were formulated. The non-poloxamer formulations served as controls, and the polymer was replaced with deionized water. The two drug concentrations were formulated to study the drug concentration effect in sol-gel transition property of poloxamer copolymer.

Evaluation of sol-gel transition property

The sol-gel transition was evaluated for poloxamer solution at skin temperature (32 °C). The poloxamer (20 % *w*/*v*) solution was prepared with deionized water and stored at 4 °C for overnight. Polypropylene microcentrifuge tube (0.25 mL; Fisher Scientific, Pittsburgh, PA) was cut towards the curved edge allowing a length of around 0.5 cm. The interior of the centrifuge tube was coated with isopropyl palmitate to impart hydrophobicity. The tip of the centrifuge tube was porated using a metal tip and placed inside an oven (32 °C) using a glass plate. About 0.1 mL of the prepared poloxamer solution was poured inside the 0.25-mL centrifuge tube through the porated site using a plastic dropper, and the setup was allowed to remain inside the oven for 10 min. The glass plate with the centrifuge tube was taken out from the oven and was examined for gelation after removal of the centrifuge tube. The image of the transitioned polymer was captured using a Proscope HR video microscope system (Hi-Scope KH 2200, Hirox Co., Tokyo, Japan).

Skin resistance and thickness testing

Porcine ear skin (Hollifield Farms, Covington, GA, USA) and dermatomed human skin (New York Fire Fighters, NY, USA) were measured for their thickness using material thickness gauge (0-1 in/0–25 mm, Electromatic Equipment Co., Inc. Cedarhurst, NY, USA). Agilent multimeter (34410A 61/2 Digit Multimeter, 33220 A 20 MHz Function/Arbitrary Waveform Generator; Agilent Technologies, Newark Element 14, Palatine, IL, USA) was used to test the resistance of skin. A frequency at 10 Hz, amplitude at 100 mV, and a resistance of 100 kΩ were used for measurements. The skin sample was placed on the receptor side of the Franz diffusion cell that was filled with pH 7.4 phosphate buffer solution, and the donor cell was clamped to the skin followed by addition of 0.3 mL phosphate buffer solution. The resistance offered by both porcine ear skin and dermatomed human skin was measured.

Scanning electron microscopy of microneedle before and after insertion

The tetrahedron-shaped solid array of maltose microneedles with 500 μm length and base width of 200 μm stacked in three rows with a total of 81 microneedles (Elegaphy Inc, Tokyo, Japan) were inserted into the porcine ear skin. Before insertion of microneedles, the skin was stretched by pulling the opposite ends using two fingers of the left hand, and by holding the base of microneedles using the forefinger and thumb of the right hand, the microneedles were inserted into the skin and held for 2 min. The duration of insertion of microneedles into the skin was selected based upon the observation that needles

get entirely dissolved inside the porated site. The Phenom Pure desktop scanning electron microscope (nanoScience Instruments, Phoenix, AZ, USA) was used to observe the microneedles before and after insertion into the skin for 2 min.

Microneedle insertion depth in the skin by confocal microscopy

The depth of microchannels created by solid maltose microneedles in the porcine ear skin was measured using a confocal microscope (Leica SP8 Microsystems, IL, USA) with an excitation wavelength of 496 nm using ×10 magnification. The skin was microporated with maltose microneedles in a similar fashion as described in scanning electron microscopy followed by application of 0.1 mL of poloxamer based 0.4 % *w*/*w* methotrexate formulation that was mixed with Fluoresoft® 0.35 % dye (20 × 0.3 mL sterile solution, Holles Laboratories, Lancaster, NY). The excess formulation was wiped off after 2 min using kimwipes followed by alcohol swabs (Covidien, Mansfield, MA, USA), and the skin was tested using confocal microscopy. The obtained images were processed using LAS-AF Software by using X-Z sectioning (Z- stack) where the depth of the microchannels was determined.

Histology examination

The microscopy of the porated skin site was tested for histology to confirm the shape and formation of in situ hydrogel microneedles. The porcine ear skin was microporated in a similar fashion that was described in the section of scanning electron microscopy followed by application of poloxamer based 0.4 % *w*/*w* methotrexate formulation that was mixed with 1 mL of methylene blue dye solution. The formulation on the skin was allowed to stand for 2 min at room temperature. The excess formulation was wiped off using kimwipes followed by alcohol swabs. The porated skin piece was stored in Tissue-Tek O.C.T Compound (Sakura Finetek USA Inc., Torrance, CA, USA) at −80 °C for overnight. The frozen skin samples were sectioned using Microm HM505E Cyrostat microtome (Southwest Scientific, USA) at around 15 μm thickness. The cryosectioned skin samples were spread on a glass slide and observed under the microscope (Leica DFC295, LAS V4.1, Leica Microsystems Inc., Buffalo Grove, IL, USA) at ×10 and ×40 magnification.

Pore visualization by methylene blue staining

The surface pore uniformity of the microchannels created by 500-μm length maltose microneedles was evaluated by methylene blue staining. The dermatomed human skin was microporated in a similar fashion that has been described in the section of scanning electron microscopy followed by application of 1 mL of methylene blue solution. The dye-treated skin was kept aside at room temperature for 2 min, and excess dye solution was removed using kimwipes and alcohol swabs. The stained microchannels in the skin were evaluated using Proscope HR video microscope system (Hi-Scope KH 2200, Hirox Co., Tokyo, Japan).

Skin rheology with microneedle treatment

The insertion of microneedle can cause skin deformation at the microporated site. The viscoelasticity of the skin can significantly influence the depth and dimension of the microchannel. In addition, the viscoelasticity of the skin can be altered based upon the type and length of microneedle, insertion duration, and poration technique. The change in the viscoelasticity property of the dermatomed human skin was determined using a rheometer (Anton Paar® GmbH, Austria-Europe) by conducting amplitude sweep followed by frequency sweep with angular frequency (ω) ranging from 100 to 0.1 rad/s. The viscoelastic parameters such as elastic property or storage (G') modulus, viscous or loss (G'') modulus, and overall change in the viscoelastic property or complex viscosity (η^*) were measured for both the untreated and in situ formed hydrogel microneedle dermatomed human skin. This test was performed to determine the difference between the viscoelasticity property of the untreated skin and skin treated with 500-μm length maltose microneedles followed by formation of in situ hydrogel microneedles.

In vitro permeation

The in vitro methotrexate permeation from 0.2 % *w*/*w* and 0.4 % *w*/*w* poloxamer and non-poloxamer-based formulations (n = 4 for each formulation) was tested with porcine ear and dermatomed human skin using vertical Franz diffusion cell (PermeGear Inc, Hellertown, PA) for 72 h. Every skin sample was tested for skin thickness and integrity before microporation as described in the section of skin resistance and thickness testing. The microporated skin was placed on the receptor chamber of the Franz diffusion cell that contains 10 mM pH 7.4 phosphate buffer solution with a magnetic stirrer at a rotational speed of 600 rpm. This receptor chamber was surrounded by water jacket maintained at 37 °C. The donor chamber was placed on the microporated skin allowing a diffusion area of 0.64 cm^2 followed by application of 100 μL formulation after 10 min equilibration. Periodic sampling (300 μL) was performed, and for every sampling time point, fresh pH 7.4 phosphate buffer solution was replaced. The passive permeation was also tested with non-porated skin for both poloxamer and non-poloxamer-based formulations since they can serve as

controls and reveal the difference in drug delivery by the in situ formed hydrogel microneedles.

HPLC analysis

The HPLC method used Waters HPLC system with a mobile phase composition of 10 mM potassium phosphate buffer adjusted to pH 3.5 and acetonitrile in the ratio of 87:13 respectively. A flow rate of 1 mL/min and UV detection at 307 nm (UV-Vis) with Waters 2996 Photodiode array detector resulted in retention time at around 3.4 min using Phenomenex Gemini-NX C18, 5 μ, (150 mm × 4.6 mm) column. The peak area of the prepared standard solution was linear with $R^2 = 1$ with a standard linear range from 0.1 to 50 μg/mL.

Statistical analysis

The statistical difference of *in vitro* permeation of methotrexate was determined using Student's *t* test. The tested formulations were considered statistically different with a probability level of 0.05 ($p < 0.05$).

Results and discussion

Evaluation of sol-gel transition property

The sol-gel transition property of poloxamer formulation has been investigated using glass microcapillary tube, magnetic stir bar, and tube inversion methods. The dehydration of poloxamer solution causes physical crosslinking and results in formation of cubic crystalline phases [24]. The change in temperature is the major driving force behind the gelation mechanism. This transition mechanism has been utilized in injectable routes where the liquid form was injected and the in situ formed gel produced sustained delivery of the encapsulated drug [24, 34]. In our study, we confirmed the sol-gel transition of poloxamer solution at skin temperature (32 °C) and this was conducted with an in-house developed method using 0.25 mL microcentrifuge tube. Figure 3a, b shows the sol-gel transition of the poloxamer (20 % *w*/*v*) solution at 32 °C and shape of pointed tip of the centrifuge tube with an even and continuous gel formation without any rugged surface. This demonstrates that poloxamer-based

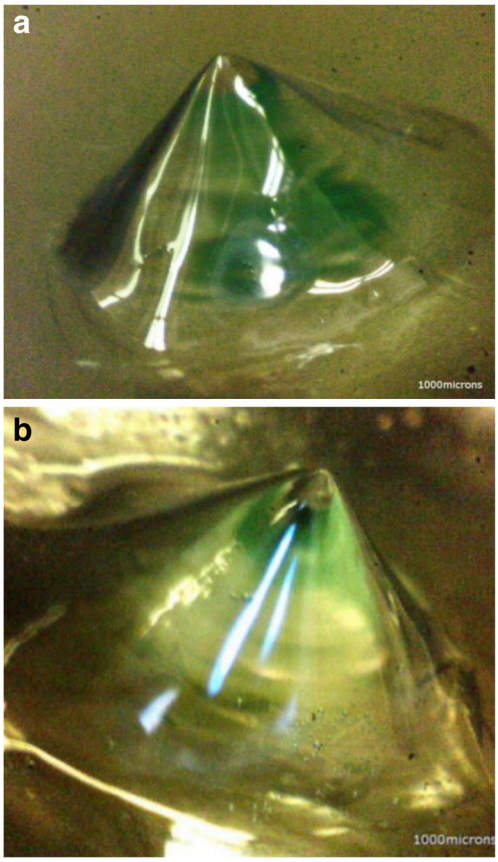

Fig. 3 Sol-gel transition property of poloxamer formulation. **a**, **b** 20.0 % *w*/*v* poloxamer solution transition to gel at 32 °C

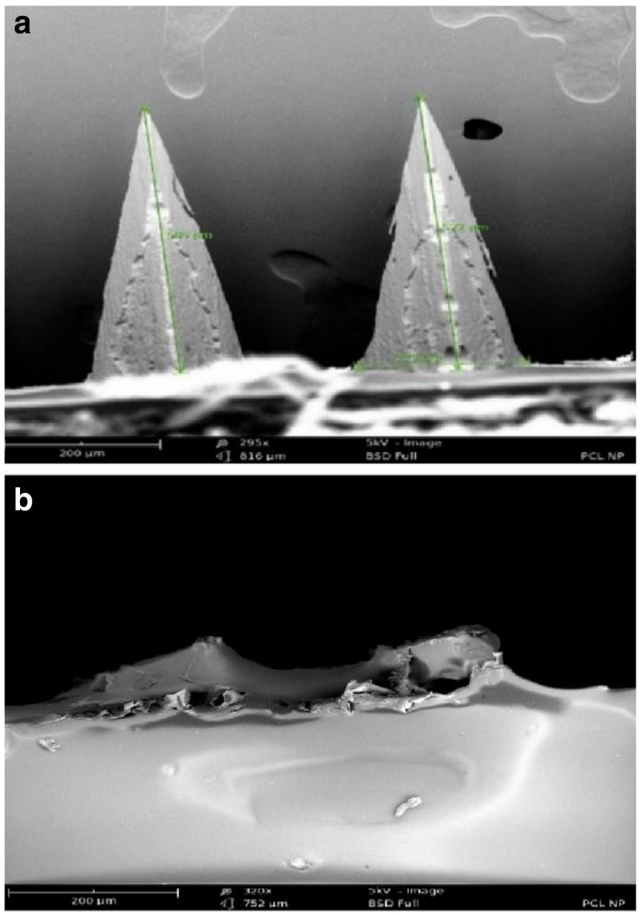

Fig. 4 Shape of maltose microneedles by scanning electron microscopy. **a** Before insertion. **b** After insertion for 2 min

formulations can transition from solution to gel at skin temperature and secure the shape of its holder.

Skin resistance and thickness testing

Skin resistance is a measurement of skin integrity [35]. As per the Organization for the Economic Cooperation and Development (OECD) guidelines, skin integrity may be compromised by improper handling. Hence, skin must be checked with a suitable method to ensure if its barrier function was maintained [36]. It is important to measure the skin integrity since it gives assurance that the skin was not compromised during cleaning or any other process. It also gives a confirmation that the alignment of skin on the Franz cell was proper and there were no perforations in the skin. The resistance of porcine ear skin and dermatomed human skin was about 20 kΩ/cm^2. The skin treated with maltose microneedles showed a 10 % decrease in resistance from its original value. The average thickness of porcine and dermatomed human skin were found to be 0.31 and 0.36 mm, respectively.

Scanning electron microscopy of microneedle before and after insertion

The microneedle insertion duration and type of insertion in the skin can play a vital role not only in depth of created microchannel but also the amount of drug delivered. The height and base width of the pyramid-shaped solid maltose microneedles from scanning electron microscopy were found to be around 500 ± 15 and 200 ± 10 μm which corresponds with the previously published data from our lab [37, 38]. The length of the microneedles decreased to 20 ± 5 μm after an insertion duration of 2 min. In case of maltose microneedles, enough insertion duration should be provided so that the microneedles can completely dissolve and form pores in the skin. Figure 4a (before insertion) and Fig. 4b (after insertion) show that the duration of 2 min insertion into the skin dissolved the maltose microneedles entirely.

Microneedle insertion depth in the skin by confocal microscopy

Microneedles are designed to bypass stratum corneum and epidermis to deliver drugs systemically. Microneedles that are made of materials such as maltose, metal, silicon, and polymers are designed with different geometry [39]. In addition to the duration and type of insertion technique as mentioned before, other factors such as pressure applied during insertion, density of material used to prepare microneedles, angle at which microneedles are inserted, viscoelastic property, and surface tension of the skin can determine the depth of microchannels. Hence, it is essential to determine the depth of microchannels in the skin created by microneedles [40].

The poloxamer based 0.4 % *w/w* methotrexate formulation with 0.2 mL Fluoresoft® 0.35 % dye was applied on the

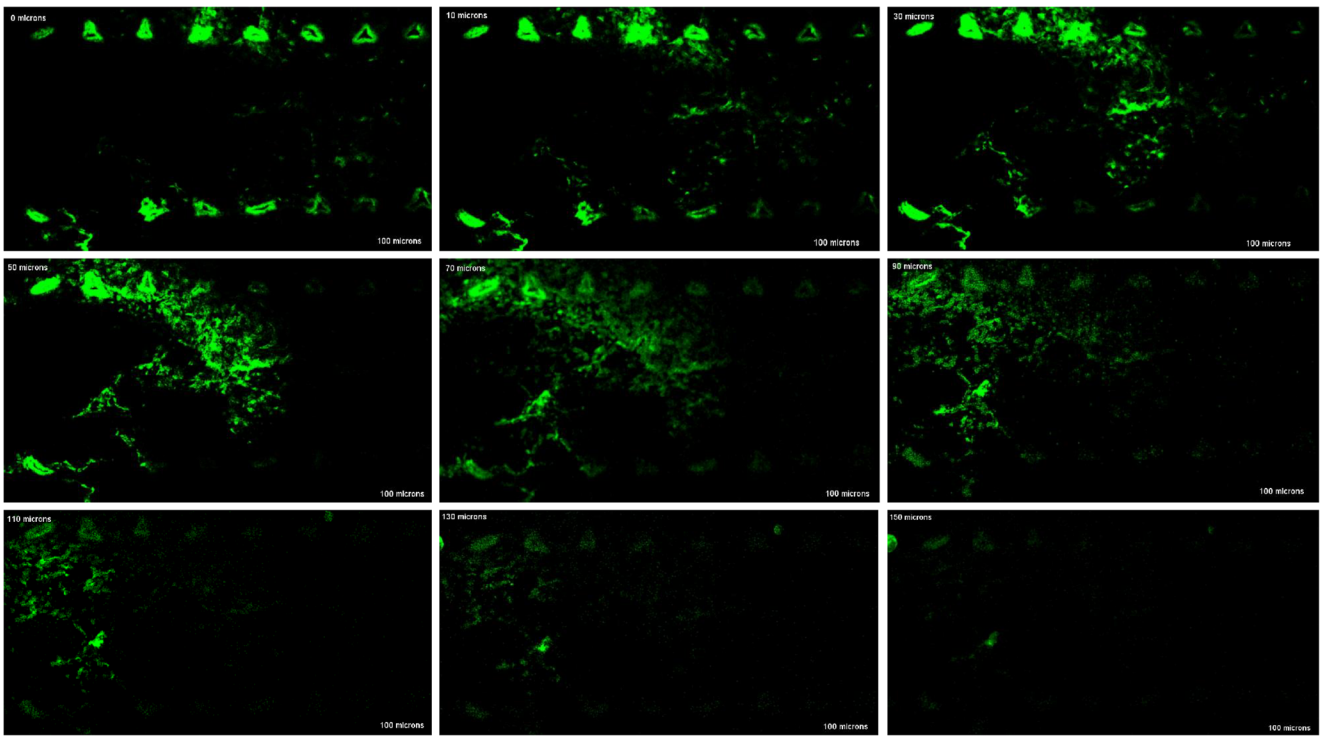

Fig. 5 Confocal microscopy images of in situ forming hydrogel microneedles. Measurement of pore depth at 0.0,10, 30, 50, 70, 90, 110, 130, and 150 μm

porated site, and the insertion depth was determined after microporation. The Z stack captures the images in sequence of skin sections at horizontal position (*x*,*y*) and at different depth (*z*) from the surface of the skin to the point at which the fluorescent dye diminish entirely [41]. In our study, it was found that the insertion of 500 μm length maltose microneedles in the porcine ear skin for a duration of 2 min resulted in pore depth of around 150 μm, as shown in Fig. 5. It can be seen from Fig. 5 that the fluorescent intensity decreased at 150 μm and this observation suggests the depth until which the applied formulation can permeate through.

Histology examination

The histology of cryosectioned skin samples is generally examined to determine the formation and shape of the microchannel [42]. Figure 6a shows that poloxamer based 0.4 % *w*/*w* methotrexate formulation with methylene blue dye solution formed a gel layer on top of the porated site of the skin. It is evident from Fig. 6b that the stratum corneum, the top layer of the skin, was ruptured followed by epidermis and allowed the formulation to flow inside the porated site before it was transitioned to gel. Further, the pyramid-shaped micropore in the skin directly reflects the shape of maltose microneedles, as shown in Fig. 4a of scanning electron microscopy section.

Pore visualization by methylene blue staining

This staining process evaluates whether the insertion duration, pressure, and geometry of the microneedles can cause even micropores in the skin. The microchannels become hydrophilic because of the presence of interstitial fluid in the skin and are stained by hydrophilic methylene blue dye solution [2]. The maltose microneedle used in our research were stacked in three rows with each row containing 27 microneedles and, hence, a total of 81 microneedles. Figure 7a, b shows untreated human skin before insertion of microneedle and even staining of microchannels after microporation respectively. The uniformity of microchannels can be determined using Pore Permeability Index (PPI) where it measures the volumetric distribution of calcein solution and analyzed by Fluoropore software. We have previously reported that the microchannels created by maltose microneedles were uniform, and it was confirmed by the bell-shaped distribution pattern of PPI histogram [37, 41].

Skin rheology with microneedle treatment

The viscoelastic properties such as G′, G″, and η* were determined to evaluate if the maltose microneedles insertion into the skin can change the viscoelastic property of skin. It was previously published from our lab that treatment of porcine ear skin with maltose microneedle, Admin Pen ™ 1200 and Admin Pen ™ 1500, resulted in decrease of storage and loss modulus [41]. The value of G′ showed a relative decrease for in situ formed hydrogel microneedle skin between 0.1 and 1 rad/s, but no

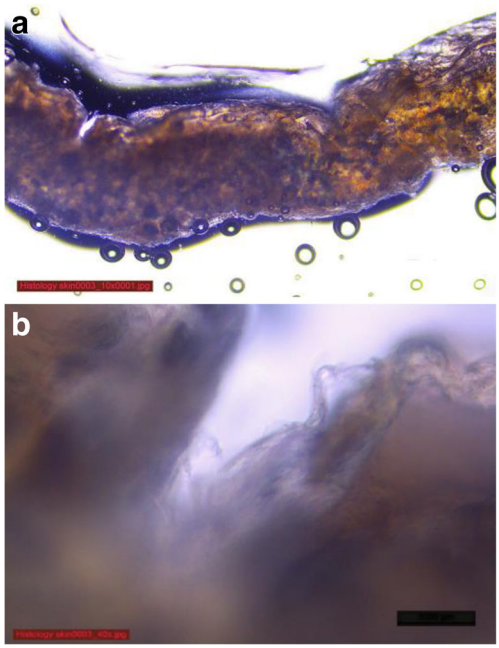

Fig. 6 Histology examination with 0.4 % *w*/*w* methotrexate poloxamer formulation (after maltose microneedles treatment). **a** Magnification at ×10. **b** Magnification at ×40

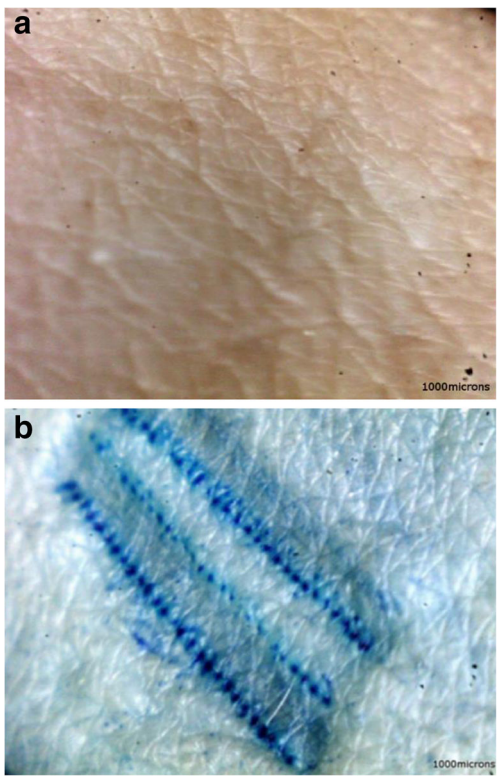

Fig. 7 Methylene blue staining for pore uniformity. **a** Untreated dermatomed human skin. **b** Methylene blue stained porated site of the dermatomed human skin by 500-μm-length maltose microneedles

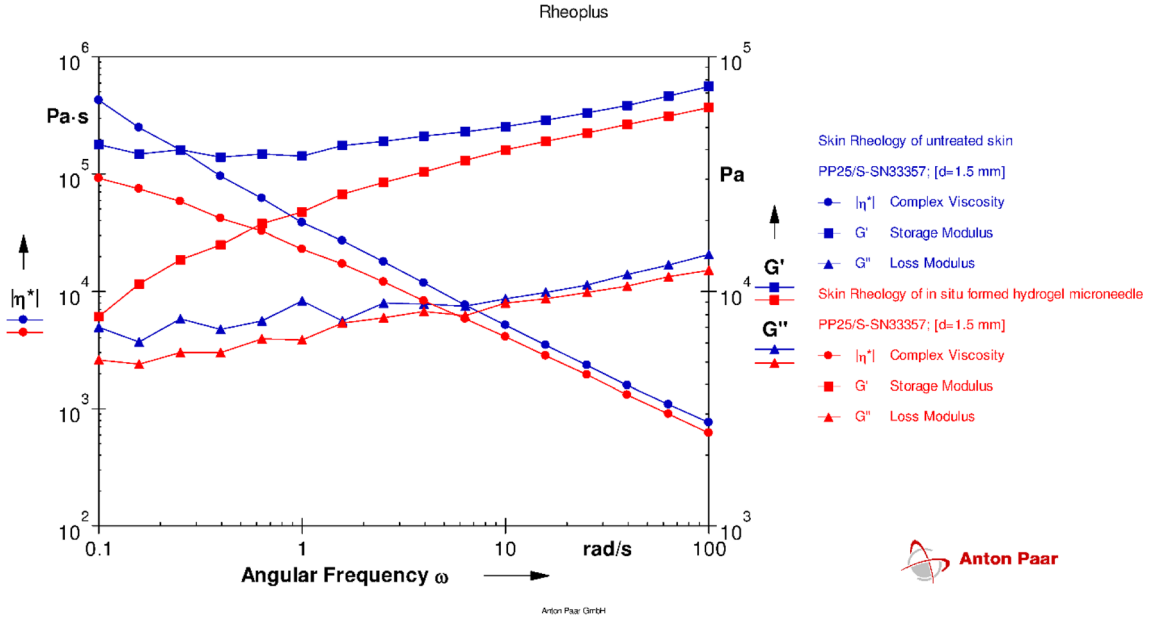

Fig. 8 Rheograms of viscoelastic parameters (G′, G″, and η*) of untreated skin and skin with in situ formed hydrogel microneedles

significant difference was observed between 1 to 100 rad/s, as shown in Fig. 8.

It can be seen from Table 1 that the values G″ and η* did not change significantly for the untreated and in situ formed hydrogel microneedles. The insertion depth (150 μm) reached by the maltose microneedles and the in situ formed hydrogel microneedles within the porated site could have contributed to the minimized overall change in the viscoelastic property of the skin.

In vitro drug permeation

The in vitro permeation of methotrexate was conducted using vertical Franz diffusion cell. The poloxamer and non-poloxamer based 0.2 % *w/w* and 0.4 % *w/w* methotrexate formulations were evaluated for drug permeation with and without microneedle treatment. The passive delivery of methotrexate served as a control and was tested to confirm if microneedle treatment followed by in situ formation of hydrogel microneedles can cause change to the delivery of methotrexate.

The poloxamer based 0.2 % and 0.4 % *w/w* methotrexate formulations delivered an average cumulative drug amount of 32.2 ± 15.76 and 114.54 ± 40.89 μg/cm^2 by the in situ formed hydrogel microneedles whereas non-poloxamer-based formulations delivered 17.19 ± 5.68 and 119.56 ± 43.72 μg/cm^2 through maltose microneedle-treated skin. The cumulative drug delivery profile (Fig. 9a, b) showed that the delivery of 0.2 % *w/w* and 0.4 % *w/w* methotrexate from non-poloxamer-based formulation was saturated after around 22 and 35 h, respectively, whereas poloxamer-based formulations at similar drug concentrations showed a continuous drug delivery profile for 72 h. A similar type of sustained drug delivery profile was observed for poloxamer based 0.2 % *w/w* and 0.4 % *w/w* methotrexate formulations as well from the flux profiles (Fig. 10a, b). The poloxamer-based formulations can act as reservoirs for drug molecules within its self-assembled micelle due to its thermogelling property at skin temperature and release the drug in a controlled fashion [43]. In our study, the in situ hydrogel microneedles formed within the microporated site showed sustained drug delivery for 72 h. The passive delivery of poloxamer and non-poloxamer based 0.2 % *w/w* and 0.4 % *w/w* methotrexate formulations delivered comparatively lesser than the microneedle-treated skin. The 0.2 % *w/w* methotrexate poloxamer and non-poloxamer-based formulations delivered 1.95 ± 1.87 and 7.65 ± 9.60 μg/cm^2, respectively, whereas the 0.4 % *w/w* methotrexate

Table 1 Rheological values of viscoelastic parameters (G′, G″, and η*) of untreated skin and skin with in situ formed hydrogel microneedles

Skin samples	Angular frequency (rad/s)	G′ storage modulus (Pa)	G″ loss modulus (Pa)	Complex viscosity [Pa·s]
Untreated skin	100	75200	14400	766
	10	50300	9270	5110
Skin with in situ formed hydrogel microneedles	100	60600	12300	619
	10	40000	8930	4100

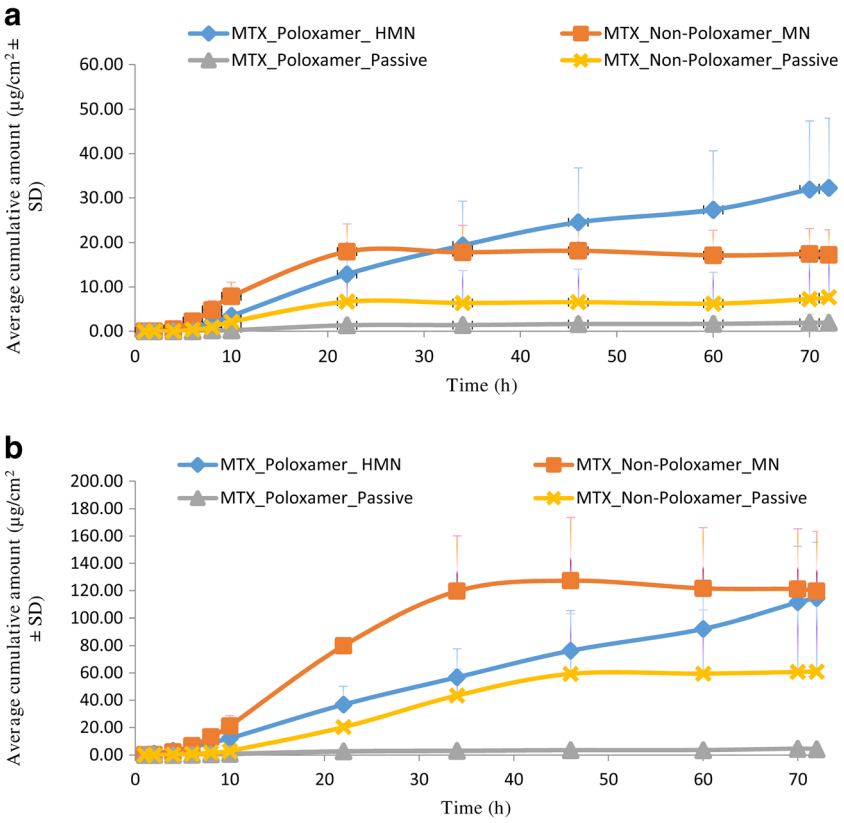

Fig. 9 In vitro average cumulative delivery profile of methotrexate by poloxamer and non-poloxamer-based formulations comparing passive and maltose microneedle-treated porcine skin. **a** Average cumulative delivery of 0.2 % *w/w* methotrexate poloxamer and non-poloxamer formulations. **b** Average cumulative delivery of 0.4 % *w/w* methotrexate poloxamer and non-poloxamer formulations. *MTX methotrexate, HMN hydrogel microneedle,MN maltose microneedle*

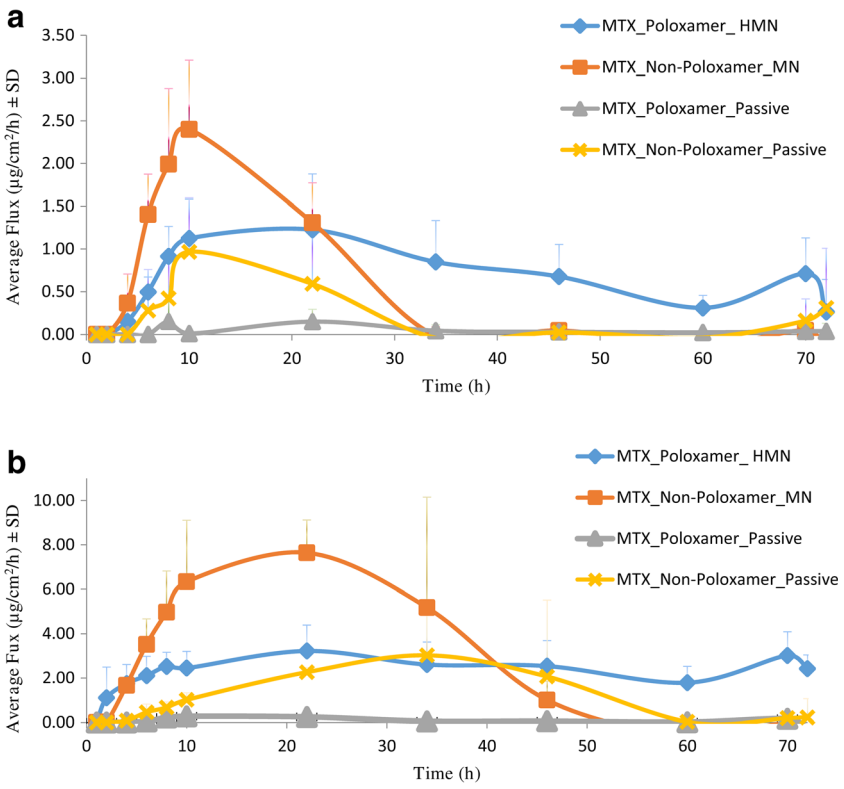

Fig. 10 In vitro average flux profile of methotrexate by poloxamer and non-poloxamer-based formulations comparing passive and maltose microneedle-treated porcine skin. **a** Average flux of 0.2 % *w/w* methotrexate poloxamer and non-poloxamer formulations. **b** Average flux of 0.4 % *w/w* methotrexate poloxamer and non-poloxamer formulations. *MTX methotrexate, HMN hydrogel microneedle, MN maltose microneedle*

poloxamer and non-poloxamer-based formulations delivered 4.15 ± 1.20 and 60.94 ± 48.81 μg/cm^2, respectively, from the passive permeation.

The poloxamer based 0.2 % *w*/*w* and 0.4 % *w*/*w* methotrexate formulations delivered 3.89 ± 0.60 and 10.27 ± 6.98 μg/cm^2, respectively, with human dermatomed skin for 72 h. The cumulative amount of drug delivered from the skin treated with maltose microneedles without the in situ hydrogel microneedles was statistically ($p < 0.05$) higher than the skin with in situ formed hydrogel microneedles. However, the drug delivery from the skin treated only with maltose microneedles tapered down entirely at around 50 h, but with the in situ formed hydrogel microneedles, the drug delivery was sustained at a low concentration.

Methotrexate delivery from porcine and human dermatomed skin confirms that the in situ formed hydrogel microneedles within the porated site caused sustained drug delivery effect. It has been reported in earlier studies that incorporation of poloxamer can facilitate solubility, encapsulation, and increased dissolution of poorly water-soluble drug molecules [34]. Further, drug crystallization and solubility can be overcome by using varying concentration of poloxamer copolymer due to formation of self-assembling micelle [44].

These novel in situ forming hydrogel microneedles have several advantages compared to other available microneedles. In case of in situ formed hydrogel microneedles, as the drug–poloxamer-based formulation was in a solution form at room temperature before application on to the skin, the formulation flowed deep inside the created microchannels, gradually transitioned to gel and resulted in formation of in situ hydrogel microneedles. It would be challenging for the formulation to flow inside the pores if the formulation is other than liquid and this may result in insufficient formation of hydrogel microneedles. The amount of drug loading within the in situ forming hydrogel microneedles is not a limitation since the formulation itself can transition at skin temperature and forms the in situ hydrogel microneedles as opposed to the dissolving microneedles where drug loading can compromise the mechanical strength of the microneedles [2]. Microneedles that are physically invasive may require safety and sterility considerations [13]. Further, microneedle fabrication requiring high melting point for polymer may pose a serious challenge for thermolabile drugs and can cause drug degradation [2]. Sterilization of microneedle may not be required for in situ forming hydrogel microneedles, but this is a common challenge among microneedles that are loaded with temperature-sensitive drugs. However, the microneedles that are used for pore formation in the skin before application of the poloxamer formulation may need to undergo sterilization if required. Further, poloxamer is a biocompatible and water-soluble polymer, and hence, using this as in situ forming hydrogel microneedles can eliminate the concern of residual biohazardous waste within the skin.

Conclusions

Microneedles with various material types and geometric dimensions have been investigated for delivery of small and large molecular weight drugs. Methotrexate has been used in treating solid tumors but is required to be delivered in a sustained fashion at low concentration because of its narrow safety margin. For the first time in our study, we have designed and evaluated novel in situ forming hydrogel microneedles using methotrexate and tested its formation as well as use in porcine ear and dermatomed human skin. Extensive characterization studies such as sol-gel transition, skin resistance and thickness, geometry of microneedle before and after insertion in the skin, depth of micropores formed inside the skin layers, histology examination for pore shape and formation, methylene blue staining for pore uniformity, viscoelasticity of untreated and microneedle treated skin, and in vitro drug permeation were carried out to confirm the formation of in situ hydrogel microneedles and deliverability of methotrexate. It can be concluded from this study that the sol-gel transition property of poloxamer-based formulation was observed in the porated site of the skin at 32 °C and the in situ formed hydrogel microneedles embedded within the microporated skin site provided a steady and sustained delivery of methotrexate.

Acknowledgments The authors would like to thank Rikhav Gala of Mercer University for his assistance with scanning electron microscopy.

Compliance with ethical standards

Conflict of interest The authors report no conflict of interest in this work.

Funding This research received no specific grant from any funding agency.

References

1. Abla MJ, Chaturvedula A, O'Mahony C, Banga AK. Transdermal delivery of methotrexate for pediatrics using silicon microneedles. Ther Deliv. 2013;4(5):543–51.
2. Tuan-Mahmood T-M, McCrudden MTC, Torrisi BM, McAlister E, Garland MJ, Singh TRR, et al. Microneedles for intradermal and transdermal drug delivery. Eur J Pharm Sci Off J Eur Fed Pharm Sci. 2013;50(5):623–37.
3. Vemulapalli V, Yang Y, Friden PM, Banga AK. Synergistic effect of iontophoresis and soluble microneedles for transdermal delivery of methotrexate. J Pharm Pharmacol. 2008;60(1):27–33.
4. Donnelly RF, McCrudden MTC, Zaid Alkilani A, Larrañeta E, McAlister E, Courtenay AJ, et al. Hydrogel-forming microneedles prepared from "super swelling" polymers combined with lyophilised wafers for transdermal drug delivery. PloS One. 2014;9(10):e111547.

5. Prausnitz MR. Microneedles for transdermal drug delivery. Adv Drug Deliv Rev. 2004;56(5):581–7.
6. Donnelly RF, Morrow DIJ, McCarron PA, David Woolfson A, Morrissey A, Juzenas P, et al. Microneedle arrays permit enhanced intradermal delivery of a preformed photosensitizer. Photochem Photobiol. 2009;85(1):195–204.
7. Li W-Z, Huo M-R, Zhou J-P, Zhou Y-Q, Hao B-H, Liu T, et al. Super-short solid silicon microneedles for transdermal drug delivery applications. Int J Pharm. 2010;389(1-2):122–9.
8. Oh J-H, Park H-H, Do K-Y, Han M, Hyun D-H, Kim C-G, et al. Influence of the delivery systems using a microneedle array on the permeation of a hydrophilic molecule, calcein. Eur J Pharm Biopharm Off J Arbeitsgemeinschaft Für Pharm Verfahrenstechnik EV. 2008;69(3):1040–5.
9. Ita K. Transdermal delivery of drugs with microneedles-potential and challenges. Pharmaceutics. 2015;7(3):90–105.
10. Gill HS, Prausnitz MR. Coated microneedles for transdermal delivery. J Control Release Off J Control Release Soc. 2007;117(2):227–37.
11. Aoyagi S, Izumi H, Fukuda M. Biodegradable polymer needle with various tip angles and consideration on insertion mechanism of mosquito's proboscis. Sens Actuators Phys. 2008;143(1):20–8.
12. Park J-H, Allen MG, Prausnitz MR. Biodegradable polymer microneedles: fabrication, mechanics and transdermal drug delivery. J Controlled Release. 2005;104(1):51–66.
13. Prausnitz MR, Langer R. Transdermal drug delivery. Nat Biotechnol. 2008;26(11):1261–8.
14. Sullivan SP, Koutsonanos DG, Del Pilar MM, Lee JW, Zarnitsyn V, Choi S-O, et al. Dissolving polymer microneedle patches for influenza vaccination. Nat Med. 2010;16(8):915–20.
15. Roxhed N, Griss P, Stemme G. Membrane-sealed hollow microneedles and related administration schemes for transdermal drug delivery. Biomed Microdevices. 2008;10(2):271–9.
16. Chandrasekaran S, Brazzle JD, Frazier AB. Surface micromachined metallic microneedles. J Microelectromechanical Syst. 2003;12(3):281–8.
17. Ovsianikov A, Chichkov B, Mente P, Monteiro-Riviere NA, Doraiswamy A, Narayan RJ. Two photon polymerization of polymer–ceramic hybrid materials for transdermal drug delivery. Int J Appl Ceram Technol. 2007;4(1):22–9.
18. Bodhale DW, Nisar A, Afzulpurkar N. Structural and microfluidic analysis of hollow side-open polymeric microneedles for transdermal drug delivery applications. Microfluid Nanofluidics. 2009;8(3):373–92.
19. Gardeniers HJGE, Luttge R, Berenschot EJW, de Boer MJ, Yeshurun SY, Hefetz M, et al. Silicon micromachined hollow microneedles for transdermal liquid transport. J Microelectromechanical Syst. 2003;12(6):855–62.
20. Martanto W, Moore JS, Couse T, Prausnitz MR. Mechanism of fluid infusion during microneedle insertion and retraction. J Control Release Off J Control Release Soc. 2006;112(3):357–61.
21. Wang PM, Cornwell M, Hill J, Prausnitz MR. Precise microinjection into skin using hollow microneedles. J Invest Dermatol. 2006;126(5):1080–7.
22. Schipper P, van der Maaden K, Romeijn S, Oomens C, Kersten G, Jiskoot W, Bouwstra J. Determination of depth-dependent intradermal immunogenicity of adjuvanted inactivated polio vaccine delivered by microinjections via hollow microneedles. Pharm Res. 2016;33(9):2269–79.
23. Garland MJ, Migalska K, Mahmood TMT, Singh TRR, Woolfson AD, Donnelly RF. Microneedle arrays as medical devices for enhanced transdermal drug delivery. Expert Rev Med Devices. 2011;8(4):459–82.
24. Dumortier G, Grossiord JL, Agnely F, Chaumeil JC. A review of poloxamer 407 pharmaceutical and pharmacological characteristics. Pharm Res. 2006;23(12):2709–28.
25. Kabanov AV, Batrakova EV, Alakhov VY. Pluronic block copolymers as novel polymer therapeutics for drug and gene delivery. J Control Release Off J Control Release Soc. 2002;82(2-3):189–212.
26. Takáts Z, Vékey K, Hegedüs L. Qualitative and quantitative determination of poloxamer surfactants by mass spectrometry. Rapid Commun Mass Spectrom RCM. 2001;15(10):805–10.
27. Dumortier G, Grossiord JL, Zuber M, Couarraze G, Chaumeil JC. Rheological study of a thermoreversible morphine gel. Drug Dev Ind Pharm. 1991;17(9):1255–65.
28. Juhasz J, Lenaerts V, Raymond P, Ong H. Diffusion of rat atrial natriuretic factor in thermoreversible poloxamer gels. Biomaterials. 1989;10(4):265–8.
29. Anderson RA. Micelle formation by oxyethylene-oxypropylene polymers. Pharm Acta Helv. 1972;47(5):304–8.
30. Attwood D, Collett JH, Tait CJ. The micellar properties of the poly(oxyethylene) - poly(oxypropylene) copolymer Pluronic F127 in water and electrolyte solution. Int J Pharm. 1985;26(1–2):25–33.
31. Bohorquez M, Koch C, Trygstad T, Pandit N. A study of the temperature-dependent micellization of Pluronic F127. J Colloid Interface Sci. 1999;216(1):34–40.
32. McDonald C, Wong CK. The effect of temperature on the micellar properties of a polyoxypropylene-polyoxyethylene polymer in water. J Pharm Pharmacol. 1974;26(7):556–7.
33. Abolmaali SS, Tamaddon AM, Dinarvand R. A review of therapeutic challenges and achievements of methotrexate delivery systems for treatment of cancer and rheumatoid arthritis. Cancer Chemother Pharmacol. 2013;71(5):1115–30.
34. Soni G, Yadav KS. High encapsulation efficiency of poloxamer-based injectable thermoresponsive hydrogels of etoposide. Pharm Dev Technol. 2014;19(6):651–61.
35. Fasano WJ, Manning LA, Green JW. Rapid integrity assessment of rat and human epidermal membranes for in vitro dermal regulatory testing: correlation of electrical resistance with tritiated water permeability. Toxicol Vitro Int J Publ Assoc BIBRA. 2002;16(6):731–40.
36. OECD. Guideline for the testing the chemicals, skin absorption: in vitro method. Adopted. 2004;13:428.
37. Kolli CS, Banga AK. Characterization of solid maltose microneedles and their use for transdermal delivery. Pharm Res. 2008;25(1):104–13.
38. Li G, Badkar A, Kalluri H, Banga AK. Microchannels created by sugar and metal microneedles: characterization by microscopy, macromolecular flux and other techniques. J Pharm Sci. 2010;99(4):1931–41.
39. Donnelly RF, Singh TRR, Garland MJ, Migalska K, Majithiya R, McCrudden CM, et al. Hydrogel-forming microneedle arrays for enhanced transdermal drug delivery. Adv Funct Mater. 2012;22(23):4879–90.
40. Yan G, Warner KS, Zhang J, Sharma S, Gale BK. Evaluation needle length and density of microneedle arrays in the pretreatment of skin for transdermal drug delivery. Int J Pharm. 2010;391(1-2):7–12.
41. Nguyen HX, Banga AK. Enhanced skin delivery of vismodegib by microneedle treatment. Drug Deliv Transl Res. 2015;5(4):407–23.
42. Kalluri H, Banga AK. Formation and closure of microchannels in skin following microporation. Pharm Res. 2011;28(1):82–94.
43. Singh-Joy SD, McLain VC. Safety assessment of poloxamers 101, 105, 108, 122, 123, 124, 181, 182, 183, 184, 185, 188, 212, 215, 217, 231, 234, 235, 237, 238, 282, 284, 288, 331, 333, 334, 335, 338, 401, 402, 403, and 407, poloxamer 105 benzoate, and poloxamer 182 dibenzoate as used in cosmetics. Int J Toxicol. 2008;27(Suppl 2):93–128.
44. Albertini B, Passerini N, Di Sabatino M, Monti D, Burgalassi S, Chetoni P, et al. Poloxamer 407 microspheres for orotransmucosal drug delivery. Part I: formulation, manufacturing and characterization. Int J Pharm. 2010;399(1-2):71–9.